Available online at www.sciencedirect.com
SCIENCE DIRECT
Journal of Solid State Chemistry 179 (2006) 1192–1201
JOURNAL OF SOLID STATE CHEMISTRY
www.elsevier.com/locate/jssc

Extended networks, porous sheets, and chiral frameworks. Thorium materials containing mixed geometry anions: Structures and properties of $Th(SeO_3)(SeO_4)$, $Th(IO_3)_2(SeO_4)(H_2O)_3 \cdot H_2O$, and $Th(CrO_4)(IO_3)_2$

Tyler A. Sullens[a], Philip M. Almond[a], Jessica A. Byrd[a], James V. Beitz[b], Travis H. Bray[a], Thomas E. Albrecht-Schmitt[a,*]

[a]*Department of Chemistry and E.C. Leach Nuclear Science Center, Auburn University, Auburn, AL 36849, USA*
[b]*Chemistry Division, Argonne National Laboratory, Argonne, IL 60439, USA*

Received 28 October 2005; received in revised form 6 January 2006; accepted 7 January 2006
Available online 7 February 2006

Abstract

Three novel Th(IV) compounds containing heavy oxoanions, $Th(SeO_3)(SeO_4)$ (**1**), $Th(IO_3)_2(SeO_4)(H_2O)_3 \cdot H_2O$ (**2**), and $Th(CrO_4)(IO_3)_2$ (**3**), have been synthesized under mild hydrothermal conditions. Each of these three distinct structures contain trigonal pyramidal and tetrahedral oxoanions. Compound **1** adopts a three-dimensional structure formed from ThO_9 tricapped trigonal prisms, trigonal pyramidal selenite, SeO_3^{2-}, anions containing Se(IV), and tetrahedral selenate, SeO_4^{2-}, anions containing Se(VI). The structure of **2** contains two-dimensional porous sheets and occluded water molecules. The Th centers are found as isolated ThO_9 tricapped trigonal prisms and are bound by four trigonal pyramidal iodate anions, two tetrahedral selenate anions, and three coordinating water molecules. In the structure of **3**, the Th(IV) cations are found as ThO_9 tricapped trigonal prisms. Each Th center is bound by six IO_3^{1-} anions and three CrO_4^{2-} anions forming a chiral three-dimensional structure. Second-harmonic generation of 532 nm light from 1064 nm radiation by a polycrystalline sample of **3** was observed. Crystallographic data (193 K, Mo$K\alpha$, $\lambda = 0.71073$): **1**; monoclinic, $P2_1/c$; $a = 7.0351(5)$ Å, $b = 9.5259(7)$ Å, $c = 9.0266(7)$ Å, $\beta = 103.128(1)$, $Z = 4$, $R(F) = 2.47\%$ for 91 parameters with 1462 reflections with $I > 2\sigma(I)$; **2**, monoclinic, $P2_1/n$, $a = 7.4889(9)$ Å, $b = 8.002(1)$ Å, $c = 20.165(3)$ Å, $\beta = 100.142(2)$, $Z = 4$, $R(F) = 4.71\%$ for 158 parameters with 2934 reflections with $I > 2\sigma(I)$; **3**, orthorhombic, $P2_12_12_1$, $a = 7.3672(5)$ Å, $b = 9.3617(6)$ Å, $c = 11.9201(7)$ Å, $Z = 4$, $R(F) = 2.04\%$ for 129 parameters with 2035 reflections with $I > 2\sigma(I)$.

Keywords: Thorium chromate; Thorium iodate; Thorium selenite; Thorium selenate; Hydrothermal crystal growth; Single crystal structure; Thermal behavior; Nonlinear optics

1. Introduction

Thorium, lacking 5*f* electrons in its normal oxidation state of +4, is ostensibly a rather mundane element compared to the heavier members of the actinide series, but has nevertheless played a number of critical roles in actinide chemistry, particularly in serving as a surrogate for more radioactive elements, especially ^{239}Pu(IV) [1]. Recently, thorium has garnered renewed interest owing to its high coordination numbers, typically eight or nine, that give rise to rich structural chemistry. Examples of these efforts include the preparation of organically templated thorium fluorides (e.g. $[C_4N_2H_{12}]_{0.5}[ThF_5]$ and $[C_5N_2H_{14}][ThF_6] \cdot 0.5H_2O$) [2], open-framework organic–inorganic hybrids, such as $[(Th_2F_5)(NC_7H_5O_4)_2(H_2O)][NO_3]$ [3], and the recent report from our group on the preparation of the first actinide tellurate in the form of the mixed-metal compound, $Th(VO_2)_2(TeO_6)(H_2O)_2$ [4].

Despite recent efforts in understanding the chemistry of U [5], Np [6], Pu [7], Am [8], and Cm [9] with oxoanions containing a nonbonding, but stereochemically active, lone-pair of electrons, little is known about the structural chemistry of thorium with anions of this type. This is

*Corresponding author. Fax: +1 334 844 6959.
E-mail address: albreth@auburn.edu (T.E. Albrecht-Schmitt).

0022-4596/$ - see front matter © 2006 Elsevier Inc. All rights reserved.
doi:10.1016/j.jssc.2006.01.017

somewhat surprising given the importance of separating and quantifying thorium via the precipitation of its iodate salt [10]. There have also been reports on the preparation and properties of thorium selenites and tellurites such as $Th(SeO_3)_2 \cdot H_2O$ [11] and $Th(TeO_3)_2$ [12] but no single-crystal X-ray diffraction data exist. The structure of $ThTe_2O_6$ has been solved using X-ray powder methods [13]. The selenite system is of particular interest because of the possibility of forming mixed-anion compounds containing both SeO_3^{2-} and SeO_4^{2-} [14], which was recently highlighted with the report of $Au_2(SeO_3)_2(SeO_4)$ [15]. Given the high coordination numbers of Th and the presence of trigonal pyramidal and tetrahedral anions there is also the distinct possibility that these compounds might adopt acentric structures [16]. Herein, we report the preparation, crystal structures, and properties of three Th(IV) compounds that contain both trigonal pyramidal and tetrahedral anions, $Th(SeO_3)(SeO_4)$ (**1**), $Th(IO_3)_2(SeO_4)(H_2O)_3 \cdot H_2O$ (**2**), and $Th(CrO_4)(IO_3)_2$ (**3**). The structures and reactivity of uranyl chromate iodates has been previously described [17].

2. Experimental

$Th(NO_3)_4 \cdot xH_2O$ (99%, Alfa-Aesar), H_5IO_6 (Alfa-Aesar), $Cr(NO_3)_3 \cdot 9H_2O$ (99.99%, Fisher), Cs_2CO_3 (99.99%, Alfa-Aesar), and H_2SeO_4 (40% aqueous soln., Alfa-Aesar) were used as received. Distilled and Millipore-filtered water with a resistance of 18.2 MΩ cm was used in all reactions. All reactions were run in PTFE-lined 23 mL Parr 4749 autoclaves. *Standard precautions for handling radioactive materials should be followed.* SEM/EDX analyses were performed using a JEOL 840/Link Isis instrument. Typical EDX analyses were within 4% of ratios determined from single crystal X-ray diffraction experiments.

2.1. $Th(SeO_3)(SeO_4)$ (1)

Cs_2CO_3 (0.171 mg, 0.526 mmol), $Th(NO_3)_4 \cdot xH_2O$ (252 mg, 0.526 mmol), H_2SeO_4 (0.33 mL, 1.28 mmol), and 0.33 mL of water were loaded in a 23 mL PTFE-lined autoclave. The autoclave was sealed and placed in a preheated furnace for 4 d at 210 °C. The furnace was then cooled at 9 °C/h to 23 °C. The product consisted of a colorless solution over colorless crystals. The major product was $Th(SeO_3)_2$. Compound **1** was present only in trace amounts and could be manually separated from $Th(SeO_3)_2$ based on differences in crystal morphology. The crystals were washed with methanol and allowed to dry. IR (KBr, cm^{-1}): 943 (ν, SeO_4^{2-}), 911 (ν, SeO_4^{2-}), 881 (ν, SeO_4^{2-}), 863 (ν, SeO_4^{2-}), 820 (ν, SeO_3^{2-}), 728 (ν, SeO_3^{2-}), 713 (ν, SeO_3^{2-}), 530, 470 (δ, SeO_3^{2-}), 442 (δ, SeO_3^{2-}), 408 (δ, SeO_4^{2-}). EDX analysis for $Th(SeO_3)(SeO_4)$ provided a Th:Se ratio of 1:2.

2.2. $Th(IO_3)_2(SeO_4)(H_2O)_3 \cdot H_2O$ (2)

$Th(NO_3)_4 \cdot xH_2O$ (145 mg, 0.291 mmol), H_5IO_6 (69 mg, 0.302 mmol), $Cr(NO_3)_3 \cdot 9H_2O$ (242 mg, 0.605 mmol), H_2SeO_4 (0.1 mL, 0.389 mmol), and 1.0 mL of water were loaded in a 23-mL PTFE-lined autoclave. The autoclave was sealed and placed in a preheated furnace for 3 d at 210 °C. The furnace was then cooled at 9 °C/h to 23 °C. The product consisted of a yellow solution over pale light-green prisms of **2** as well as microcrystalline aggregates of at least two unidentified byproducts. The solids were washed with methanol, and allowed to dry. Crystals of **2** were manually separated from the other solids. Yield: 76 mg (33% based on Th). IR (KBr, cm^{-1}): 3547 (ν, H_2O), 3466 (ν, H_2O), 1653 (δ, H_2O), 1612 (δ, H_2O), 1588 (δ, H_2O), 900 (ν, SeO_4^{2-}), 867 (ν, SeO_4^{2-}), 853 (ν, SeO_4^{2-}), 817 (ν, IO_3^{1-}), 802 (ν, IO_3^{1-}), 785 (ν, IO_3^{1-}), 760 (ν, IO_3^{1-}), 715 (ν, IO_3^{1-}), 600 (δ, IO_3^{1-}), 532 (δ, IO_3^{1-}). EDX analysis for $Th(IO_3)_2(SeO_4)(H_2O)_3 \cdot H_2O$ provided a Th:I:Se ratio of 1:2:1.

2.3. $Th(CrO_4)(IO_3)_2$ (3)

$Th(NO_3)_4 \cdot xH_2O$ (217 mg, 0.435 mmol), H_5IO_6 (103 mg, 0.451 mmol), $Cr(NO_3)_3 \cdot 9H_2O$ (181 mg, 0.451 mmol), and 1.0 mL of water were loaded in a 23-mL PTFE-lined autoclave. The autoclave was sealed and placed in a preheated furnace for 3 d at 200 °C. The furnace was then cooled at 9 °C/h to 23 °C. The product consisted of a yellow solution over orange-yellow prisms. Yield: 300 mg, near quantitative. The crystals were washed with methanol and allowed to dry. Phase purity was confirmed by comparing the X-ray powder diffraction pattern with the pattern calculated from single crystal data. IR (KBr, cm^{-1}): 958 (ν, CrO_4^{2-}), 925 (ν, CrO_4^{2-}), 908 (ν, CrO_4^{2-}), 853 (ν, CrO_4^{2-}), 809 (ν, IO_3^{1-}), 790 (ν, IO_3^{1-}), 780 (ν, IO_3^{1-}), 735 (ν, IO_3^{1-}), 714 (ν, IO_3^{1-}), 595 (δ, IO_3^{1-}), 544 (δ, IO_3^{1-}). EDX analysis for $Th(CrO_4)(IO_3)_2$ provided a Th:Cr:I ratio of 1:1:2.

2.4. Nonlinear optical measurements

Powder second harmonic generation (SHG) measurements were performed on a Kurtz–Perry nonlinear optical system [18] as modified by Porter and co-workers [19] and updated here to include laser pulse energy normalization. A Q-switched Nd:YAG laser (Continuum Surelite I-10), operated at 10 Hz, provided the 1064 nm light used for all measurements. The SHG intensity was recorded from the as-synthesized thorium compound and from fine ground α-quartz (crystalline SiO_2). These powders were placed in separate glass tubes of the same dimensions. No index of refraction matching fluid was used in these experiments. The SHG light at 532 nm was collected in reflection, selected by a narrow band-pass interference filter (Pomfret) and detected by a photomultiplier tube (RCA 1P28). A near normal incidence beam splitter reflected a small fraction of the laser beam onto a pyroelectric detector (Molectron J3-05) that was used as a laser pulse energy monitor. A digital storage oscilloscope (Tektronix TDS 640A) signal averaged and recorded both the SHG and incident laser energy signals. Average laser power was measured separately with a calibrated Scientech volume

Table 1
Crystallographic data for $Th(SeO_3)(SeO_4)$ (**1**), $Th(IO_3)_2(SeO_4)(H_2O)_3 \cdot H_2O$ (**2**), and $Th(CrO_4)(IO_3)_2$ (**3**)

Formula	$Th(SeO_3)(SeO_4)$	$Th(IO_3)_2(SeO_4)(H_2O)_3 \cdot H_2O$	$Th(CrO_4)(IO_3)_2$
Formula mass (amu)	501.96	796.86	697.84
Space group	$P2_1/c$ (No. 14)	$P2_1/n$ (No. 14)	$P2_12_12_1$ (No. 19)
a (Å)	7.0351(5)	7.4889(9)	7.3672(5)
b (Å)	9.5259(7)	8.002(1)	9.3617(6)
c (Å)	9.0266(7)	20.165(3)	11.9201(7)
α (deg)	90	90	90
β (deg)	103.128(1)	100.142(2)	90
γ (deg)	90	90	90
V (Å^3)	589.11(8)	1189.6(3)	822.12(9)
Z	4	4	4
T (°C)	−80	−80	−80
λ (Å)	0.71073	0.71073	0.71073
ρ_{calcd} (g/cm^3)	5.660	4.404	5.638
μ(Mo$K\alpha$) (cm^{-1})	376.48	208.56	269.38
$R(F)$ for $F_o^2 > 2\sigma(F_o^2)$[a]	0.0247	0.0471	0.0204
$R_w(F_o^2)$[b]	0.0565	0.1165	0.0423

[a] $R(F) = \sum||F_o| - |F_c||/\sum|F_o|$.
[b] $R_w(F_o^2) = [\sum[w(F_o^2 - F_c^2)^2]/\sum wF_o^4]^{1/2}$.

absorber calorimeter. The observed SHG intensity per unit laser intensity, $I^{2\omega}$, was obtained by dividing the SHG signal by the laser energy signal. Replicate measurements determined the value of interest for the sample compound, $I^{2\omega}$ (s), and for α-quartz, $I^{2\omega}$ (q). The ratio of these values, $I^{2\omega}$ (s)/$I^{2\omega}$ (q), was found to be (0.25 ± 0.03) at an incident laser intensity of 17 MW/cm^2. This provides evidence that the SHG efficiency of $Th(CrO_4)(IO_3)_2$ (**3**) is comparable to that of α-quartz, a material frequently used to determine the relative SHG performance of nonlinear optical materials.

2.5. Thermal analysis

Thermal data for **2** and **3** were collected using a TA Instruments, Model 2920 Differential Scanning Calorimeter (DSC) and a TA Q50 Thermogravimetric Analyzer (TGA). Samples (~10 mg) were encapsulated in aluminum or platinum pans and heated at 10 °C/min from 25 to 600 °C under a nitrogen atmosphere.

2.6. Crystallographic studies

Crystals of $Th(SeO_3)(SeO_4)$ (**1**), $Th(IO_3)_2(SeO_4)(H_2O)_3 \cdot H_2O$ (**2**), and $Th(CrO_4)(IO_3)_2$ (**3**) were mounted on glass fibers with epoxy and aligned on a Bruker SMART APEX CCD X-ray diffractometer. Intensity measurements were performed using graphite monochromated Mo$K\alpha$ radiation from a sealed tube and a monocapillary collimator. SMART was used for preliminary determination of the cell constants and data collection control. For all compounds, the intensities of reflections of a sphere were collected by a combination of three sets of exposures (frames). Each set had a different φ angle for the crystal and each exposure covered a range of 0.3° in ω. A total of 1800 frames were collected with an exposure time per frame of 40 s for **1**, 60 s for **2**, and 30 s for **3**. Longer exposure times for **1** and **2** were necessary due to the small size of the crystals.

For **1**–**3**, determination of integrated intensities and global cell refinement were performed with the Bruker SAINT software package using a narrow-frame integration algorithm. A face-indexed numerical absorption correction was initially applied using XPREP [20]. Individual shells of unmerged data were corrected and exported in the same format. These files were subsequently treated with a semi-empirical absorption correction by SADABS [21]. The program suite SHELXTL was used for space group determination (XPREP), direct methods structure solution (XS), and least-squares refinement (XL) [20]. Some crystallographic details are listed in Table 1. Additional details can be found in the Supporting Information.

3. Results and discussion

3.1. Syntheses

The hydrothermal reaction of $Th(NO_3)_4 \cdot xH_2O$ with selenic acid results in the reduction of Se(VI) to Se(IV) and the subsequent crystallization of $Th(SeO_3)_2$ with trace amounts of $Th(SeO_3)(SeO_4)$ (**1**). We have obtained better crystals from this reaction when Cs_2CO_3 is added to the starting mixture. This reaction presumably proceeds via the oxidation of water. Unlike sulfate, selenate is a reasonably strong oxidizing agent with $E^\circ = 1.151$ V. Alternatively, the selenate anion might be undergoing thermal decomposition under hydrothermal conditions to yield selenite [22]. Yields of **1** were not improved by changing the reaction conditions, scale, or stoichiometry. The preparation of $Th(IO_3)_2(SeO_4)(H_2O)_3 \cdot H_2O$ (**2**) is less than straightforward. In this case, $Th(NO_3)_4 \cdot xH_2O$ is reacted with H_5IO_6, $Cr(NO_3)_3 \cdot 9H_2O$, and H_2SeO_4 to yield the

desired product. The periodic acid is reduced yielding iodate ($E^\circ = 1.601$ V), which is a convenient method for slowly introducing iodate in *f*-element reactions [23–25], the Cr(III) is also oxidized to Cr(VI) (requiring 1.2–1.3 V) and remains in solution, and finally the selenic acid remains SeO_4^{2-} in this reaction owing to the presence of the strongly oxidizing IO_6^{5-}. The preparation of $Th(CrO_4)(IO_3)_2$ (**3**) is the most direct, involving the oxidation of Cr(III) to CrO_4^{2-} by IO_6^{5-} with concomitant reduction to IO_3^{1-}. These then crystallize with Th(IV) to yield **3** in near quantitative yield.

3.2. Structure of $Th(SeO_3)(SeO_4)$ (*1*)

This compound adopts a three-dimensional structure formed from ThO_9 tricapped trigonal prisms, trigonal pyramidal selenite, SeO_3^{2-}, anions containing Se(IV), and tetrahedral selenate, SeO_4^{2-}, anions containing Se(VI), as is shown in Fig. 1. The ThO_9 polyhedra edge-share to form one-dimensional chains that extend down the *a*-axis. Each selenate anion bridges between three such chains. The selenite anion chelates one thorium center in one chain and uses its third oxygen atom to bridge to a second chain. A view of the extended structure is depicted in Fig. 2.

Th–O bond distances, which range from 2.354(5) to 2.625(5) Å, are within the normal limits, with the two longest Th–O bond distances (2.530(4) and 2.625(5) Å) being with the two μ_3-O atoms of the selenite anions, O(5) and O(6), respectively. The selenate bond distances (Se(1)–O) range from 1.625(5) to 1.638(5) Å, with O–Se(1)–O bond angles ranging from 106.9(2)° to 113.0(2)°. Se(2)–O bonds occur from 1.677(5) to 1.734(5) Å, with O–Se(2)–O bond angles from 91.1(2)° to 103.8(2)°. Selected bond distances for **1** can be found in Table 2. Bond-valence sum calculations yielded values of 4.14 for Th(1), 6.10 for Se(1), and 3.93 for Se(2), which are in agreement with the formal oxidation states [26,27].

3.3. $Th(IO_3)_2(SeO_4)(H_2O)_3 \cdot H_2O$ (*2*)

The structure of $Th(IO_3)_2(SeO_4)(H_2O)_3 \cdot H_2O$ contains two-dimensional sheets extending in the [*bc*] plane and occluded water molecules. The Th centers are found as isolated ThO_9 tricapped trigonal prisms being bound by four trigonal pyramidal iodate anions, two tetrahedral selenate anions, and three coordinating water molecules. All four IO_3^{1-} anions coordinate to Th on the same side of the ThO_9 units in an approximately fourfold pattern

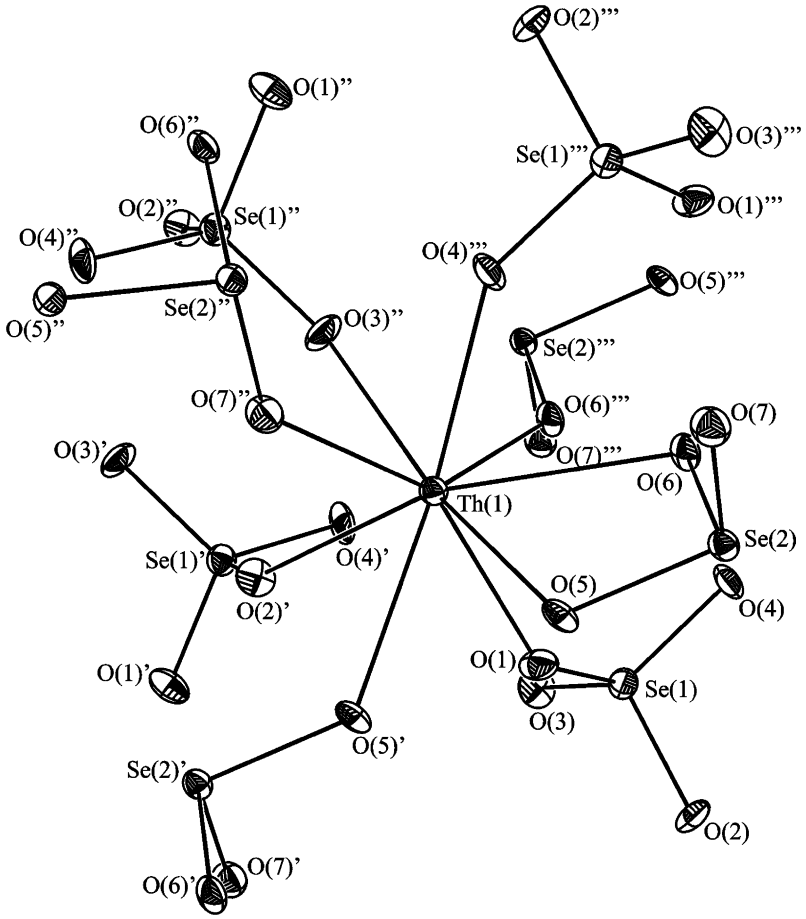

Fig. 1. A view of the fundamental building units in $Th(SeO_3)(SeO_4)$ (**1**) showing ThO_9 tricapped trigonal prisms, trigonal pyramidal selenite, SeO_3^{2-}, anions containing Se(IV), and tetrahedral selenate, SeO_4^{2-}, anions containing Se(VI). 50% probability ellipsoids are depicted.

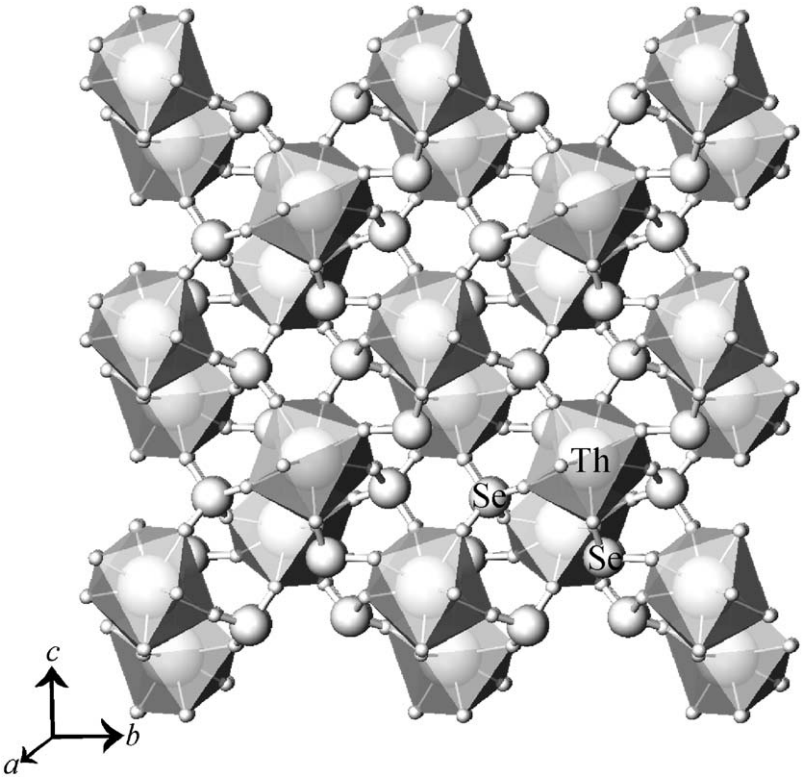

Fig. 2. A depiction of the extended structure of $Th(SeO_3)(SeO_4)$ (**1**).

Table 2
Selected bond distances (Å) for $Th(SeO_3)(SeO_4)$ (**1**)

Th(1)–O(1)	2.404(5)	Th(1)–O(7)′	2.354(5)
Th(1)–O(2)′	2.426(5)	Se(1)–O(1)	1.625(5)
Th(1)–O(3)′	2.458(5)	Se(1)–O(2)	1.626(5)
Th(1)–O(4)′	2.464(5)	Se(1)–O(3)	1.638(5)
Th(1)–O(5)	2.458(5)	Se(1)–O(4)	1.638(5)
Th(1)–O(5)′	2.530(4)	Se(2)–O(5)	1.677(5)
Th(1)–O(6)	2.625(5)	Se(2)–O(6)	1.725(4)
Th(1)–O(6)′	2.429(5)	Se(2)–O(7)	1.734(5)

through two capping and two *trans* trigonal prismatic oxygen atoms, as is shown in Fig. 3. The two remaining trigonal prismatic oxygen atoms on one side of the ThO_9 units are from the two SeO_4^{2-} anions. Th(1)–O bond distances range from 2.383(7) to 2.611(7) Å with the longest three distances being those to the coordinated water molecules. These water molecules are directed between the layers. The sheets of **2** are porous with gaps on the order of 15.76×5.50 Å (Fig. 4). The stacking of these sheets is shown in Fig. 5. The occluded water molecule is located between the sheets and is in close proximity to the pores in the sheets. A number of interactions exist between the water molecules and oxygen atoms in the layers that are of appropriate length for hydrogen bonding interactions. These O···O interactions range from 2.638(7) to 3.196(7) Å, 2.723(7) to 3.271(7) Å, and 2.626(7) to 3.084(7) Å, for O(11), O(12), and O(13), respectively. The occluded water molecule, O(14), also possesses several potential hydrogen bonding interactions with distances ranging from 2.877(7) to 3.143(7) Å.

There are two crystallographically unique IO_3^{1-} anions in the structure of **2**. The iodate anion containing I(1) caps the ThO_9 unit, while the iodate containing I(2) occupies some of the sites forming the trigonal prism. Each iodate anion has a terminal oxygen atom. The I(1)–O bond lengths range from 1.797(7) to 1.819(8) Å, and those of I(2) occur from 1.800(7) to 1.817(8) Å. The O–I–O bond angles for the two IO_3 units are also nearly identical with ranges of 95.7(4)° to 98.9(4)° for I(1) and 95.4(4)° to 98.0(4)° for I(2). There are also interactions between an oxygen atom of an iodate anion in one layer with the iodine atom of an iodate in another layer. These contacts are on the order of 2.6 Å. Even longer contacts can be observed if tolerances are extended out to 3.3 Å, making both iodate anions IO_{3+4} units. These interactions are commonly found in iodate compounds and are often used to stitch low-dimensional features together [23,28–32]. The SeO_4^{2-} anions bridge two ThO_9 units and also have two terminal oxygen atoms. Bond lengths within this unit range from 1.608(8) to 1.644(8) Å, and the bond angles from 106.7(4)° to 111.6(4)°. Selected bond distances for **2** can be found in Table 3. The bond-valence sums are as follows: Th(1), 4.27; Se(1), 6.23; I(1), 5.06; and I(2), 5.03 [26,27].

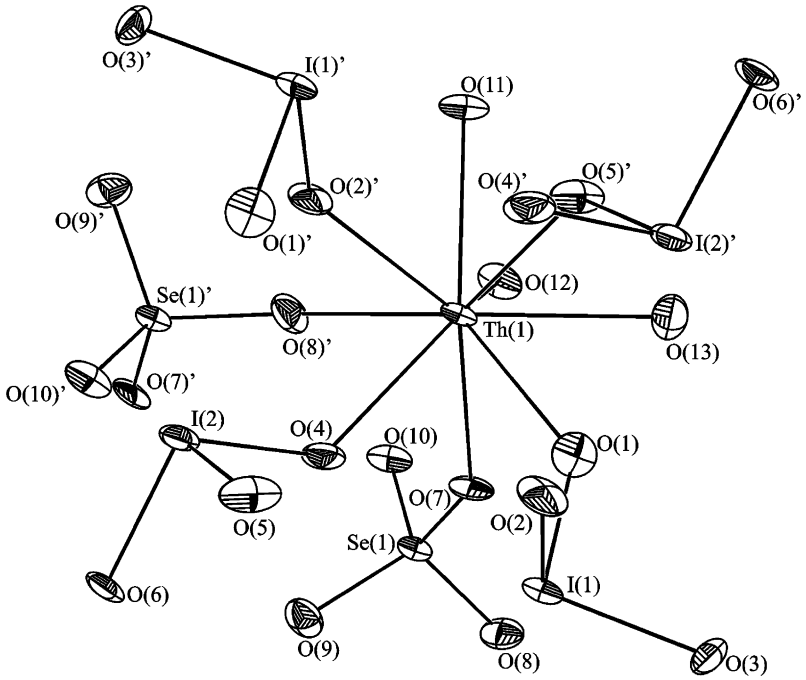

Fig. 3. An illustration of the ThO_9, IO_3^{1-}, and SeO_4^{2-} units in $Th(IO_3)_2(SeO_4)(H_2O)_3 \cdot H_2O$ (**2**). 50% probability ellipsoids are depicted.

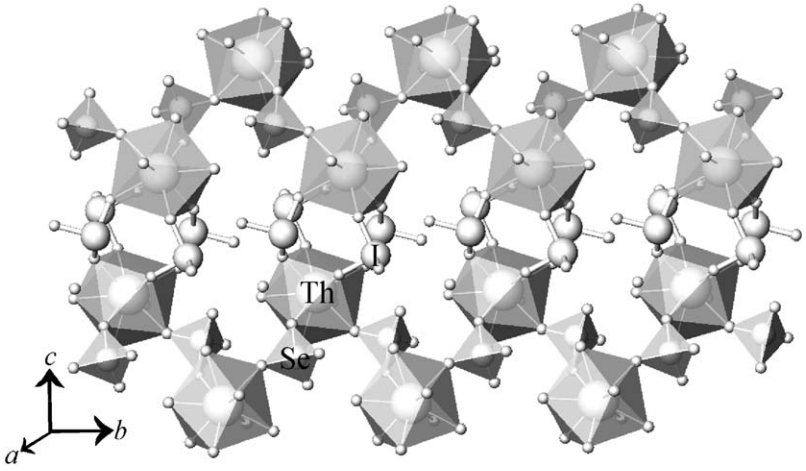

Fig. 4. A view down the *a* axis of the porous sheets in $Th(IO_3)_2(SeO_4)(H_2O)_3 \cdot H_2O$ (**2**).

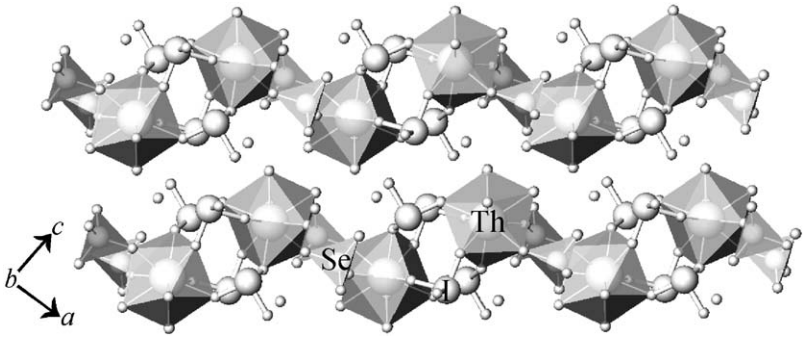

Fig. 5. A depiction of the stacking sequence of the $Th(IO_3)_2(SeO_4)(H_2O)_3$ layers in **2** with interstitial water.

3.4. $Th(CrO_4)(IO_3)_2$ (3)

As in **1** and **2**, the Th(IV) cations in **3** are found as ThO_9 tricapped trigonal prisms. Each Th center is bound by six IO_3^{1-} anions and three CrO_4^{2-} anions (Fig. 6). The Th–O distances range from 2.345(5) to 2.670(5) Å, with no correlation between Th–O bond length and ligand type. Compound **3** crystallizes in the chiral space group $P2_12_12_1$, possibly owing to the presence of the lone-pair of electrons on the iodate anions. Although this feature is also present in **1** and **2**, both of these compounds are centrosymmetric. It is predicted, based on the acentric crystal class of **3**, that this compound should exhibit the second-harmonic generation of laser light. This property was tested for by irradiating a polycrystalline sample of **3** with 1064 nm laser light. The generation of 532 nm light was clearly observed providing verification that this compound is indeed acentric. Both the $I(1)O_3^{1-}$ and $I(2)O_3^{1-}$ trigonal pyramidal units bridge between three ThO_9 units. The CrO_4^{2-} anions also corner-share with three ThO_9 units. The remaining oxygen atom on the CrO_4^{2-} anion is terminal. The coordination of the CrO_4^{2-} anions to Th(IV) yields $[ThCrO_4]$ sheets that propagate in the [*ab*] plane. The thorium atoms are then further coordinated by the iodate anions that link the sheets together to create a three-dimensional structure as shown in Fig. 7.

Table 3
Selected bond distances (Å) for $Th(IO_3)_2(SeO_4)(H_2O)_3 \cdot H_2O$ (**2**)

Distances (Å)			
Th(1)–O(1)	2.427(8)	I(1)–O(2)	1.819(8)
Th(1)–O(2)′	2.427(8)	I(1)–O(3)	1.797(7)
Th(1)–O(4)	2.430(8)	I(2)–O(4)	1.817(8)
Th(1)–O(5)′	2.416(8)	I(2)–O(5)	1.810(7)
Th(1)–O(7)	2.383(7)	I(2)–O(6)	1.800(7)
Th(1)–O(8)′	2.385(8)	Se(1)–O(7)	1.644(8)
Th(1)–O(11)	2.463(8)	Se(1)–O(8)	1.608(8)
Th(1)–O(12)	2.611(7)	Se(1)–O(9)	1.624(8)
Th(1)–O(13)	2.496(8)	Se(1)–O(10)	1.621(8)
I(1)–O(1)	1.805(9)		

The I–O bond lengths for the two iodate anions range from 1.794(5) to 1.827(5) Å. The $I(1)O_3^{1-}$ anion is more uniform than the $I(2)O_3^{1-}$ anion and has O–I(1)–O bond angles ranging from 94.5(3)° to 98.8(3)°; whereas the $I(2)O_3^{1-}$ anion has O–I(2)–O bond angles from 92.8(2)° to 100.6(2)°. Cr–O bond lengths are consistent with literature values [19], ranging from 1.616(5) to 1.664(5) Å, with the terminal O(3) atom having the expected shortest bond length to Cr(1). The CrO_4^{2-} anions are close to idealized tetrahedral symmetry with O–Cr–O bond angles ranging from 107.7(3)° to 111.0(3)° Selected bond distances for **3** can be found in Table 4. The bond-valence sums of the central atoms in this compound are 4.32 for Th(1), 5.97 for Cr(1), 5.19 for I(1), and 4.93 for I(2), which are consistent with the expected oxidation states [26,27].

While there are no known naturally occurring thorium minerals containing iodate or selenite, there are at least two chromate iodate minerals, dietzeite, $Ca_2H_2O(IO_3)_2(CrO_4)$

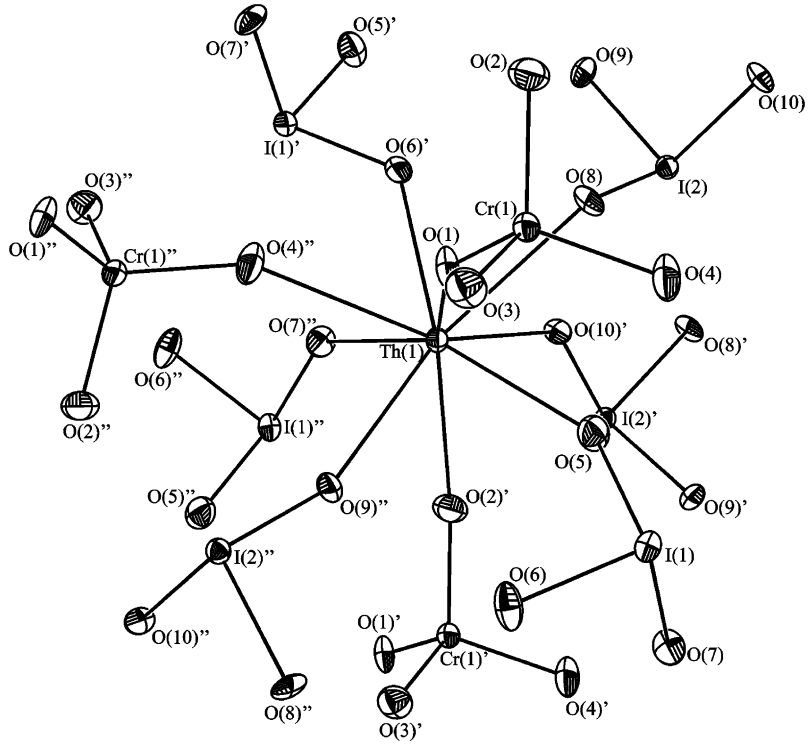

Fig. 6. A depiction of the fundamental building units in $Th(CrO_4)(IO_3)_2$ (**3**) showing a Th center bound by six IO_3^{1-} anions and three CrO_4^{2-} anions. 50% probability ellipsoids are depicted.

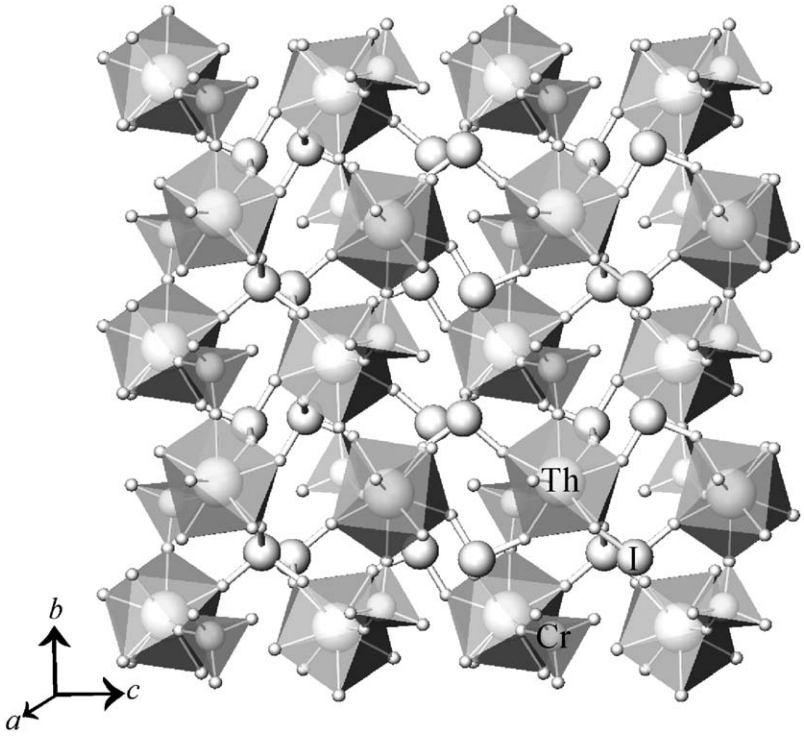

Fig. 7. An illustration of the extended structure of $Th(CrO_4)(IO_3)_2$ (**3**) showing [$ThCrO_4$] sheets that propagate in the [*ab*] plane. These sheets are linked together by iodate anions to create a chiral three-dimensional structure.

Table 4
Selected bond distances (Å) for $Th(CrO_4)(IO_3)_2$ (**3**)

Th(1)–O(1)	2.382(5)	Cr(1)–O(2)	1.663(5)
Th(1)–O(2)′	2.670(5)	Cr(1)–O(3)	1.616(5)
Th(1)–O(4)′	2.547(5)	Cr(1)–O(4)	1.642(5)
Th(1)–O(5)	2.345(5)	I(1)–O(5)	1.794(5)
Th(1)–O(6)′	2.402(5)	I(1)–O(6)	1.803(5)
Th(1)–O(7)′	2.408(5)	I(1)–O(7)	1.795(5)
Th(1)–O(8)	2.526(5)	I(2)–O(8)	1.809(5)
Th(1)–O(9)′	2.361(5)	I(2)–O(9)	1.812(5)
Th(1)–O(10)′	2.418(5)	I(2)–O(10)	1.827(5)
Cr(1)–O(1)	1.664(5)		

[31], and georgericksenite, $Na_6CaMg(IO_3)_6(CrO_4)_2(H_2O)_{12}$ [32], two sulfate iodates, hectorfloresite, $Na_9(IO_3)(SO_4)_4$ [33], and fuenzalidaite, $K_6(Na,K)_4Na_6Mg_{10}(SO_4)_{12}(IO_3)_{12} \cdot 12H_2O$ [34], and a selenate iodate, carlosruizite, $K_6(Na,K)_4Na_6Mg_{10}(SeO_4)_{12}(IO_3)_{12} \cdot 12H_2O$ [34]. In georgericksenite, analyses indicate some sulfur substitution occurs at the Cr site, making this mineral a sulfate chromate iodate. These minerals point to new directions in mixed-anion chemistry.

3.5. Thermal behavior

The thermal behavior of $Th(IO_3)_2(SeO_4)(H_2O)_3 \cdot H_2O$ (**2**) was evaluated primarily to investigate the temperatures of water loss and decomposition. A DSC thermogram of **2** reveals endotherms at 116, 192, 262, 296, 447, 537, and 564 °C. The first endotherm is minor, and corresponds to the loss of water absorbed onto the surface of the crystals. This is followed by the removal of lattice water at 192 °C. The coordinating water molecules are lost in distinct steps near 262 and 296 °C. Then it appears that the selenate anion thermally decomposes to yield selenite with the loss of oxygen at 447 °C [22]. At 537 °C, the onset of the final decomposition of **2** occurs in the temperature range expected for iodate disproportionation [23], with appropriate weight loss for the removal of I_2 from the sample. It is interesting to note that there are two separate decomposition events near 500 °C that may indicate that each of the crystallographically unique iodate anions in this compound decompose at slightly different temperatures.

The thermal behavior of $Th(CrO_4)(IO_3)_2$ (**3**) is much more straightforward with a single endotherm corresponding to disproportionation of iodate occurring at 543 °C. This decomposition temperature is very similar to that of $Th(IO_3)_2(SeO_4)(H_2O)_3 \cdot H_2O$ (**2**).

4. Conclusions

In this report we have demonstrated that the structural chemistry of thorium with mixed heavy oxoanions is diverse and rich with previously unknown structure types. The high coordination number of Th(IV), nine-coordinate in the compounds reported herein, provides an ideal platform for constructing solids with both layered and chiral networks. It is noteworthy that one does not solely

obtain humdrum, centrosymmetric, three-dimensional structures as one might have predicted to occur with Th(IV) and anions of this type. Given current trends in transition metal and uranyl selenite and selenate chemistry [35], particularly with organic templates [36], it might be of interest to explore the effects of replacing four-, five- and six-coordinate transition metals with eight- and nine-coordinate actinides, like thorium.

Auxiliary material: Further details of the crystal structure investigations may be obtained from the Fachinformationzentrum Karlsruhe, D-76344 Eggenstein-Leopoldshafen, Germany (Fax: +49 7247 808 666; *E-mail address*: crysdata@fiz-karlsruhe.de) on quoting depository numbers CSD 415808, 415807, and 415806.

Acknowledgment

This work was supported by the Chemical Sciences, Geosciences and Biosciences Division, Office of Basic Energy Sciences, Office of Science, Heavy Elements Program, US Department of Energy under Grant DE-FG02-01ER15187 at Auburn University and under Contract W-31-109-ENG-38 at Argonne National Laboratory.

References

[1] N. Dacheux, A.C. Thomas, B. Chassigneux, V. Brandel, M. Genet, Ceram. Trans. 93 (1999) 373.
[2] J.-Y. Kim, A.J. Norquist, D. O'Hare, Chem. Commun. 19 (2002) 2198.
[3] J.-Y. Kim, A.J. Norquist, D. O'Hare, J. Am. Chem. Soc. 125 (2003) 12688.
[4] T.A. Sullens, T.E. Albrecht-Schmitt, Inorg. Chem. 44 (2005) 2282.
[5] (a) P.M. Almond, T.E. Albrecht-Schmitt, Am. Miner. 89 (2004) 976; (b) P.M. Almond, T.E. Albrecht-Schmitt, Inorg. Chem. 42 (2003) 5693.
[6] (a) E. Jobiliong, Y. Oshima, J.S. Brooks, T.E. Albrecht-Schmitt, Solid State Commun. 132 (2004) 337; (b) P.M. Almond, R.E. Sykora, S. Skanthakumar, L. Soderholm, T.E. Albrecht-Schmitt, Inorg. Chem. 43 (2004) 958; (c) T.E. Albrecht-Schmitt, P.M. Almond, R.E. Sykora, Inorg. Chem. 42 (2003) 3788.
[7] (a) A.C. Bean, B.L. Scott, T.E. Albrecht-Schmitt, W. Runde, J. Solid State Chem. 176 (2004) 1346; (b) A.C. Bean, B.L. Scott, T.E. Albrecht-Schmitt, W. Runde, Inorg. Chem. 42 (2003) 5632; (c) W. Runde, A.C. Bean, T.E. Albrecht-Schmitt, B.L. Scott, Chem. Commun. 4 (2003) 478.
[8] (a) W. Runde, A.C. Bean, B.L. Scott, Chem. Commun. 15 (2003) 1848; (b) R.E. Sykora, Z. Assefa, R.G. Haire, T.E. Albrecht-Schmitt, Inorg. Chem. 44 (2005) 5667.
[9] R.E. Sykora, Z. Assefa, R.G. Haire, T.E. Albrecht-Schmitt, J. Solid State Chem. 177 (2004) 4413.
[10] (a) T.J. Tranter, T.A. Todd, L.C. Lewis, J.P. Henscheid, US Pat. Appl. Publ. 2004, US 2004052705; (b) R. Collee, Can. J. Chem. 46 (1968) 1691; (c) Yu.A. Chernikhov, T.A. Uspenskaya, Zavod. Lab. 9 (1940) 276.
[11] V.P. Nesterenko, V.P. Glybin, Czech. J. Phys. 49 (1999) 903.
[12] Yu.G. Mashirov, V.B. Yadrintsev, Radiokhimiya 24 (1982) 256.
[13] M.L. Lopez, M.L. Veiga, A. Jerez, C. Pico, J. Less-Common Met. 175 (1991) 235.
[14] (a) H. Effenberger, Miner. Petrol. 36 (1987) 3; (b) G. Giester, Monatsh. Chem. 120 (1989) 661; (c) R.E. Morris, A.P. Wilkinson, A.K. Cheetham, Inorg. Chem. 31 (1992) 4774; (d) I. Krügermann, M.S. Wickleder, Z. Anorg. Allg. Chem. 628 (2002) 147; (e) M. Weil, U. Kolitsch, Acta Crystallogr. C 58 (2002) 47; (f) J. Baran, T. Lis, M. Marchewka, H. Ratajczak, J. Mol. Struct. 250 (1991) 13; (g) G. Giester, Monatsh. Chem. 123 (1992) 957; (h) W.T.A. Harrison, Z. Zhang, Eur. J. Solid State Inorg. Chem. 34 (1997) 599; (i) S.V. Krivovichev, I.G. Tananaev, V. Kahlenberg, B.F. Myasoedov, Dokl. Phys. Chem. 403 (2005) 124.
[15] M.S. Wickleder, O. Buechner, C. Wickleder, S. el Sheik, G. Brunklaus, H. Eckert, Inorg. Chem. 43 (2004) 5860.
[16] P.S. Halasyamani, K.R. Poeppelmeier, Chem. Mater. 10 (1998) 2753.
[17] (a) R.E. Sykora, D.M. Wells, T.E. Albrecht-Schmitt, Inorg. Chem. 41 (2002) 2304; (b) R.E. Sykora, S.M. McDaniel, D.M. Wells, T.E. Albrecht-Schmitt, Inorg. Chem. 41 (2002) 5126.
[18] S.K. Kurtz, T.T. Perry, J. Appl. Phys. 39 (1968) 3798.
[19] Y. Porter, K.M. Ok, N.S.P. Bhuvanesh, P.S. Halasyamani, Chem. Mater. 13 (2001) 1910.
[20] G.M. Sheldrick, SHELXTL PC, Version 6.12, An Integrated System for Solving, Refining, and Displaying Crystal Structures from Diffraction Data, Siemens Analytical X-ray Instruments, Inc., Madison, WI, 2001.
[21] G.M. Sheldrick, SADABS 2001, program for absorption correction using SMART CCD based on the method of Blessing: R.H. Blessing, Acta Crystallogr. A 51 (1995) 33.
[22] D. Havlicek, Z. Micka, R. Boublikova, Coll. Czech. Chem. Commun. 60 (1995) 969.
[23] A.C. Bean, S.M. Peper, T.E. Albrecht-Schmitt, Chem. Mater. 13 (2001) 1266.
[24] A.L. Hector, S.J. Henderson, W. Levason, M. Webster, Z. Anorg. Allg. Chem. 628 (2002) 198.
[25] P. Douglas, A.L. Hector, W. Levason, M.E. Light, M.L. Matthews, M. Webster, Z. Anorg. Allg. Chem. 630 (2004) 479.
[26] I.D. Brown, D. Altermatt, Acta Crystallogr. B 41 (1985) 244.
[27] N.E. Brese, M. O'Keeffe, Acta Crystallogr. B 47 (1991) 192.
[28] A.C. Bean, T.E. Albrecht-Schmitt, J. Solid State Chem. 161 (2001) 416.
[29] A.C. Bean, M. Ruf, T.E. Albrecht-Schmitt, Inorg. Chem. 40 (2001) 3959.
[30] S.C. Abrahams, J.L. Bernstein, J.B.A.A. Elemans, G.C. Verschoor, J. Chem. Phys. 59 (1973) 2007.
[31] P.C. Burns, F.C. Hawthorne, Can. Miner. 31 (1993) 313.
[32] M.A. Cooper, F.C. Hawthorne, A.C. Roberts, J.D. Grice, J.A.R. Stirling, E.A. Moffatt, Am. Miner. 83 (1998) 390.
[33] G.E. Ericksen, H.T. Evans Jr., M.E. Mrose, J.J. McGee, J.W. Marinenko, J.A. Konnert, Am. Miner. 74 (1989) 1207.
[34] J.A. Konnert, H.T. Evans Jr., J.J. McGee, G.E. Ericksen, Am. Miner. 79 (1994) 1003.
[35] (a) S.V. Krivovichev, V. Kahlenberg, I.G. Tananaev, R. Kaindl, E. Mersdorf, B.F. Myasoedov, J. Am. Chem. Soc. 127 (2005) 1072; (b) S.V. Krivovichev, V. Kahlenberg, R. Kaindl, E. Mersdorf, I.G. Tananaev, B.F. Myasoedov, Angew. Chem. Int. Ed. 44 (2005) 1134; (c) T.E. Albrecht-Schmitt, Angew. Chem. Int. Ed. 44 (2005) 4836; (d) P.M. Almond, T.E. Albrecht-Schmitt, Inorg. Chem. 42 (2003) 5693; (e) Y. Porter, P.S. Halasyamani, J. Solid State Chem. 174 (2003) 441; (f) K.M. Ok, P.S. Halasyamani, Chem. Mater. 14 (2002) 2360; (g) Y. Porter, P.S. Halasyamani, Inorg. Chem. 40 (2001) 2640.

[36] (a) C.N.R. Rao, M. Dan, J.N. Behera, Pure Appl. Chem. 77 (2005) 1655;
(b) D. Udayakumar, M. Dan, C.N.R. Rao, Eur. J. Inorg. Chem. 8 (2004) 1733;
(c) I. Pasha, A. Choudhury, C.N.R. Rao, J. Solid State Chem. 174 (2003) 386;
(d) D. Udayakumar, C.N.R. Rao, J. Mater. Chem. 13 (2003) 1635;
(e) I. Pasha, A. Choudhury, C.N.R. Rao, Solid State Sci. 5 (2003) 257;
(f) I. Pasha, A. Choudhury, C.N.R. Rao, Inorg. Chem. 42 (2003) 409.